Such nodules may represent fossil coprolites in which the phosphate is derived from organic residues. Zangerl and Richardson (1963) described apatite-bearing coprolites with a light to dark brown structureless groundmass, which they assumed to be collophane. A non-concretionary origin is implicit.

Ames (1959) synthesized apatite by replacement of calcite in 0.3M Na_3PO_4 and analysed samples at intervals. Material approximating to francolite could be obtained by this method but he found no evidence for the inclusion of CO_3^{2-} into the apatite lattice when it was crystallized from solution. He concluded that the formation of marine phosphorites by diagenetic replacement of Ca CO_3 was feasible in Ca-saturated water with PO_4^{3-} > 0.1µg/ml and pH > 7.0.

Gluskoter et al. (1970) demonstrated early replacement of cellulose by carbonate fluorapatite in a petrified log in black shales but there are no recorded instances where direct precipitation of francolite from solution under geological conditions has been proved.

In the present case the petrographic and microprobe evidence shows that francolite is present as cryptocrystalline matrix material in which detrital micas and other layer silicate grains are partly orientated. The siderite spherulites do not appear to be replacive and probably formed very early in the diagenetic history of these clay-rich sediments. A kaolinite X-ray fabric study on a sideritic concretion from the same sequence (Oertel and Curtis, 1972) showed near-random orientation at the concretion centre indicating that siderite growth began in uncompacted sediment. It may be therefore that in concretion 33 the matrix crystallized slightly later but still in relatively watery sediment since the acid insoluble residue is no higher than average and no obvious distortion or oriented flakes around the siderites can be seen.

A coprolite origin is improbable. Whilst the absence of any gastric charactersitics may be explained by destructive phosphate replacement, the similarity of the quartz : kaolinite : mica of the residue with that of the host shale suggests a common origin. All concretions in the sequence show phosphate enrichment relative to the shale, yet, with the exception of a cone-in-cone concretion, calcite is absent. The latter concretion is of undoubted late diagenetic (post-compactional) origin and thus a replacement mechanism seems not unreasonable. Early concretional and perhaps also some detrital calcite was probably replaced as PO_4^{3-} concentration increased in the pore water with degradation of basic proteins in the organic rich sediment. Such putrefaction would tend to maintain the high pH necessary for francolite formation.

Knowles (1963) in an investigation of phosphatic nodules of the same age from nearby exposure proposed on the basis of Uranium enrichment that the phosphate was syngenetic with the sediment : ion exchange took place while the collophane pellets rolled to and fro on the sea bed. This can almost certainly be discounted in the present case as concretion 33 was taken from immediately below the seat earth in the probable non-marine 'blue clays'.

Microprobe X-ray scanning photographs clearly have great potential in textural studies on fine grained sediments and it is anticipated that work currently in progress on other concretionary minerals and host sediments will provide valuable information on diagenetic reactions.

Acknowledgements. I thank Sheila Lindsay for the fluorine analyses and George Taylor for help with the electron microprobe. Walter Ritchie and Alexander Reid produced the photographs and Wilma Hadden prepared the manuscript.

REFERENCES

Altschuler (Z.S.), Gisney (E.A.), and Barlow (I.H.), 1953. Amer.Mineral. 38, 328.

Ames (L.L.Jr.), 1959. Econ.Geol. 54, 829.

Brophy (G.P.) and Nash (J.T.), 1968. Amer.Mineral. 53, 445.

Brown (G.), 1961. The X-ray identification and crystal structures of clay minerals. Mineralogical Society, London.

Clements (R.L.), Sergeant (G.A.), and Webb (P.J.), 1971. Analyst, 96, 51.

Deans (T.), 1938. Mineral Mag. 25, 135.

Deer (W.A.), Howie (R.A.), and Zussman (J.), 1962. Rock forming minerals. 5, 323. Longmans, London.

Gluskoter (H.J.), Pierard (L.H.), and Pfefferkorn (H.W.), 1970. Jour.Sed. Petrol. 40, 1363.

Knowles (B.), 1963. Proc.Yorks.Geol.Soc. 34, 413.

McConnell (D.), 1952. Bull.Soc.franc.Mineral.Crist. 75, 428.

, 1960. Amer.Mineral. 45, 209.

Neuman (W.F.), and Neuman (M.W.), 1953. Chem.Revs. 53, 1

Oertel (G.) and Curtis (C.D.), 1972. Geol.Soc.America Bull. 83, 2597.

Pearson (M.J.), 1973. The geochemistry of a Westphalian Sediment Sequence. Ph.D. thesis, University of Sheffield.

- , 1974a. Mineral.Mag. 39, 696.

- , 1974b. Mineral.Mag. 39, 700.

Sandell (E.B.), Hey (M.H.), and McConnell (D.), 1939. Mineral.Mag. 25, 395.

Thewlis (J.), Glock (G.E.), and Murray (M.N.), 1939. Trans.Faraday.Soc. 35, 358.

Zangerl (R.) and Richardson (E.S.Jr.), 1963. Fieldiana: Geology Memoirs 4. Chicago Nat. Hist. Mus.

F.Scordari: Ferrinatrite (Appendix—H-bonding)

The crystal structure of ferrinatrite and its relationships to Maus' salt, by F.Scordari (this vol., pp. 375-83

Appendix: Hydrogen bonds. The six hydrogen atoms belong to three independent water molecules, shared among Na polyhedra. They could not be located from a difference Fourier synthesis. Positions assigned on purely geometric criteria and on a combination of geometric and valency-balance criteria are not incomplete agreement in respect of the hydrogen bonds to one of the three water molecules: purely geometric criteria suggest that Aq(3) is hydrogen-bonded to O(7,3) and O(5) or O(5,4), while when valency-balance is taken into account bonds to O(6) and O(11) or O(2,3) seem more probable.

From geometric considerations of the interatomic distances and angles (Table II, p.) Aq(2) has three distances less than 3.2Å, corresponding to possible hydrogen bonds, but of the three angles between these vectors, two are outside the acceptor - donor - acceptor range suggested by Ferraris and Franchini-Angela (1972); the most probable bonding is therefore O(7,4) - Aq(2) - O(5,3). For Aq(1), which has several suitable distances and acceptor - donor - acceptor angles, hydrogen bonds to O(12) and O(12,4) are the most likely, since O(12) is only shared by S(3) tetrahedra. For Aq(3) the most probable configurations from purely geometrical considerations are O(7,3) - Aq(3) - O(5,4) and O(7,3) - Aq(3) - O(5).

Electrostatic valency-balance calculations were carried out using the bond:strength:bond-length relation given by Brown and Shannon (1973) and the curve of bond-valencies reported by Donnay and Donnay (1973). Taken together with the geometrical considerations, they support the above conclusions concerning the bonding of Aq(1) and Aq(2), but for Aq(3) either O(6) - Aq(3) - O(11) or O(6) - Aq(3) - O(2,3) leads to a better balance.

All other possible configurations have been examined, but neither the purely geometric nor the geometric plus valency-balance considerations are in full agreement with the total electrostatic valency balance on the oxygen atoms. The geometrical criterion leads to O(7) and O(5) being much overbonded and O(6) much underbonded for O(7,3) - Aq(3) - O(5,4). On the other hand application of both geometric and valency-balance criteria leads to O(8) being underbonded and Aq(1), Aq(2), and Aq(3) overbonded for O(6) - Aq(3) - O(11). Similar arguments may be brought forward for O(7,3) - Aq(3) - O(5) and O(6) - Aq(3) - O(2,3).

Thirdly, if we consider the electrostatic valency balance alone, the best balance is given by bonds from Aq(1) to O(8,2) and O(12,4), from Aq(2) to O(12) and O(7), and from Aq(3) to O(6) and O(5,4).

In Table IV the valency balance is summarized on all three criteria; the differences do not seem sufficient to make a definite decision.

Table IV. Electrostatic valence balance: E, on valence-balance criteria only, assuming Aq(1) bonded to O(8,2) and O(12,4), Aq(2) to O(12) and O(7), and Aq(3) to O(6) and O(5,4); G, on geometric criteria alone, assuming Aq(1) bonded to O(12) and O(12,4), Aq(2) to O(7,3) and O(5,3), and Aq(3) to O(7,3) and O(5,4); GE, and valence-balance and geometric criteria jointly, assuming Aq(1) and Aq(2) bonded as under G, but Aq(3) bonded to O(6) and O(11).

Atom	Fe	S	Na(1)	Na(2)	Na(3)	E H‖	E Sum	G H‖	G Sum	GE H‖	GE Sum
O(1)	0.50†	1.42††	-	-	-	-	1.92	-	1.92	-	1.92
O(2)	0.50†	1.42**	-	-	-	-	1.92	-	1.92	-	1.92
O(3)	0.49*	1.38**	-	0.17	-	-	2.04	-	2.04	-	2.04
O(4)	0.51*	1.36††	0.17	-	-	-	2.04	-	2.04	-	2.04
O(5)	-	1.65**	-	0.06	0.18	0.17	2.06	{0.11 0.17	2.17	0.11	2.00
O(6)	-	1.55**	0.10	0.11	-	0.14	1.90	-	1.76	0.13	1.89
O(7)	-	1.61††	{0.06 0.20	-	-	0.17	2.04	{0.16 0.13	2.16	0.16	2.03
O(8)	-	1.61††	0.09	0.11	-	0.13	1.94	-	1.81	-	1.81
O(9)	0.50‡	1.43‡‡	-	-	-	-	1.93	-	1.93	-	1.93
O(10)	0.50‖	1.39‡‡	-	-	{0.14 0.09	-	2.08	-	2.08	-	2.08
O(11)	-	1.52‡‡	-	0.14	{0.11 0.14	-	1.91	-	1.91	0.12	2.03
O(12)	-	1.66‡‡	-	-	-	{0.17 0.17	2.00	{0.12 0.17	1.95	{0.12 0.17	1.95
Aq(1)	-	-	0.21	-	0.18	{0.87 0.83	2.09	{0.88 0.83	2.10	{0.88 0.83	2.10
Aq(2)	-	-	0.17	0.22	-	{0.83 0.83	2.05	{0.89 0.84	2.12	{0.89 0.84	2.12
Aq(3)	-	-	-	0.19	0.20	{0.86 0.83	2.08	{0.87 0.83	2.09	{0.87 0.88	2.14
Sum	3.00	18.00	1.00	1.00	1.00	6.00	30.00	6.00	30.00	6.00	30.00

* Fe(1); † Fe(2); ‡ Fe(3); ‖ Fe(4); ** S(1); †† S(2); ‡‡S(3);

H‖ The hydrogen atoms are, of course, members of Aq(1), Aq(2), and Aq(3), and linked by "hydrogen bonds" to O(5) to O(12)

REFERENCES

Brown (I.D.) and Shannon (R.D.), 1973. Acta Crystallogr. A29, 266

Donnay (G.) and Donnay (J.D.H.), 1973. Ibid. B29, 1417

Ferraris (G.) and Franchini-Angela (M.), Ibid. B28, 3572

N.M.S.Rock: Fenite from Loch Borrolan

A new occurrence of fenite from the Loch Borrolan alkaline complex, Assynt.

N.M.S.Rock, Dept.of Mineralogy and Petrology, Downing Site, Cambridge

The notoriously poor exposure of the Borrolan complex has necessitated exposure mapping of its complex petrology (Woolley, 1970). Fenitized quartzites have been reported from three restricted localities in its NW, NE, and SE extremities (Woolley et al., 1972), and this communication completes the intermittent fenite halo with a fourth single occurrence in the SW corner. This new rock differs curiously from both these previous fenites and from all known Borrolan igneous rocks, exposed or revealed by recent drilling (D.W.Matthews and A.R.Woolley, pers.comm.).

The three fenites reported earlier are associated with potassic pseudo-leucite-bearing syenites (borolanites and potassic veins), but this new occurrence is among pyroxene-hornblende syenites ("appinites of Woolley, 1970) near to the celebrated cromaltite (biotite pyroxenite), which represents an isolated and restricted mass of a more extensive ultramafic sheet buried beneath the peat (Matthews and Woolley, 1976). As with these previous fenites, field relations are obscure: the type is restricted to a single moss-covered blue-grey boulder among pyroxene-hornblende syenite outcrops on the far side of Bad na h'Achlaise from the cromaltite (fig.1), perhaps margining the apophysis from the Basal Cambrian quartzite sheet, which lies on the Assynt thrust. The boulder comprises highly porous (though tough) fibrous fine-grained rock, which in thin section is an inhomogeneous combination of stubby greenish pyroxene prisms and feebly pleochroic amphibole either in subhedral prisms with ragged terminations or rounded sub-radiating fibrous masses, with apatite abundant in patches and minor

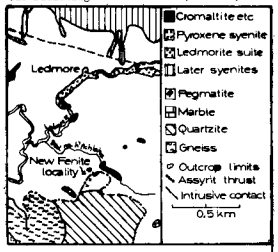

Fig.1. Location of the new fenite locality in the SW corner of the Loch Borralan complex, Assynt. Figure adapted from Matthews and Woolley (1976).

The petrography and optics of the pyroxene and amphibole need not be detailed as they are similar to those in the fenitized quartzites of Woolley et al. (1972).

Average Energy-dispersive microprobe analyses of these constituent minerals are shown in Table I. The feldspar shows no visible exsolution, unlike many fenite feldspars (McKie, 1966, etc.), but is optically inhomogeneous, being mostly untwinned but sometimes revealing poorly-developed microcline tartan; the inhomogeneity is structural rather than compositional, since the probe reveals practically no zoning. No albite was detected. The chlorine content of the apatites was below the limit of microprobe detection (ca. 0.1%). The pyroxene is a rather diopsidic aegirine-augite varying from $Di_{47}Hd_7Ac_{46}$ to $Di_{33}Hd_5Ac_{62}$ - not a typically igneous composition (fig.2), but lying between the fields of previously analysed Borralan fenite pyroxenes and other pyroxenes from fenitised granitic gneisses (Sokli and E.Uganda). All these Al-poor pyroxenes are interesting because they span a region in which there are no igneous compositions, in which zoning is usually intense, and where an immiscibility field between diopsidic and acmite-rich pyroxenes has been conjectured. Future work may indicate whether they are true homogeneous structures or fine-scale exsolutions. The amphibole lies just within the field of richterite as defined by Leake (1968) with Mg/(Mg+Fe) varying between 72.0 and 77.5%. Note that the rather high Si per 23 oxygens is due to calculation of the total iron as FeO; treatment of the Fe in the manner used for the other Borralan amphiboles by Woolley et al. (1972) reduces the Si below 8.

Mineral compositions in this new fenite, then, are closely comparable with previous Borralan examples, which carry orthoclase, richterite, diopsidic pyroxene, and apatite, but the new rock lacks their quartz, biotite, and albite, while other amphibole species reported (actinolite, crossite, and riebeckite) are not seen. The mode is also entirely different; though difficult to estimate quantitatively because the fenite is a combination of pure pyroxene and amphibole segregations rather than a homogeneous mixture, this is estimated at 30-55% pyroxene, 25-60% amphibole, 7-10% apatite, and 1-6% feldspar, with 5-20% porosity, whereas the most mineralogically-similar fenitized quartzites carry 26-46% feldspar, 9-54% quartz, andonly 16-42% pyroxene plus amphibole (Woolley et al., 1972). Consequently the bulk composition must differ considerably - unfortunately the specimen pores were filled with such tenacious vegetable and mineral impurities that it proved impossible to prepare a satisfactory powder for analysis, and an analysis would in any case have little value, bearing in mind the inhomogeneity. Nevertheless, as the CIPW norms of the constituent minerals show 1% (pyroxene) and 8% (amphibole) quartz (with total iron partitioned suitably into FeO and Fe_2O_3), the bulk fenite must be nearly saturated, whereas the previous examples carried 14 to 52% normative quartz.

The field relations of this fenite, even if it is in situ, are equivocal: if the fenitizing pyroxene-hornblende syenite belongs to the earlier (ledmorite) suite of the Borralan complex, which predated the Assynt thrust (Woolley, 1970), it might have formed either from the basal Cambrian quartzite now outcropping adjacently, or from whatever country rock lay in that position - the outcrop could lie on either side of the thrust plane. Conversely, if the pyroxene-hornblende syenite belongs to the later Cnoc na'Sroine nordmarkite, which postdates the thrust, a quartzite parent is most likely.

Table I. Average microprobe compositions of fenite minerals, Borralan.

	1	2		4	5	6
SiO_2	65.65	0.75	54.08	54.55	57.32	57.04
TiO_2	Nil	Nil	Nil	0.13	Nil	0.22
Al_2O_3	18.31	Nil	0.25	Nil	Nil	Nil
FeO*	0.40	Nil	16.11	20.32	11.29	10.20
MnO	Nil	Nil	0.27	0.22	0.26	0.27
MgO	Nil	Nil	8.47	6.18	16.91	17.37
CaO	Nil	54.00	13.66	9.91	4.34	4.63
Na_2O	0.43	Nil	6.35	8.78	6.08	6.26
K_2O	15.85	Nil	Nil	Nil	0.88	1.20
P_2O_5	-	41.27	-	-	-	-
	100.64	96.02	99.19	100.09	97.08	97.19
O =	8	12	6	6	23	23
Si	3.009	0.062	2.084	2.112	8.029	8.156
Ti	-	-	-	0.004	-	0.023
Al	0.989	-	0.011	-	-	-
Fe	0.015	-	0.519	0.659	1.350	1.220
Mn	-	-	0.009	0.007	0.031	0.032
Mg	-	-	0.486	0.357	3.608	3.701
Ca	-	4.732	0.564	0.412	0.666	0.710
Na	0.038	-	0.474	0.660	1.689	1.736
K	0.927	-	-	-	0.160	0.218
P	-	2.858	-	-	-	-
Total	4.978	7.562	4.147	4.211	15.712	15.796

1. Interstitial microcline ($Or_{95.6-96.2}$); two analyses.
2. Chlorine-poor apatite.
3. Most magnesian pyroxene (core zone).
4. Most alkaline pyroxene (two analyses).
5. Most iron-rich amphibole (two anals.).
6. Most magnesian amphibole (two anals.).

* Total iron as FeO

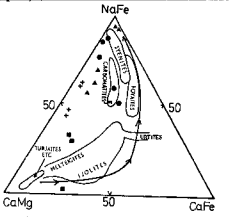

Fig.2. Plot of pyroxenes from fenites and alkaline igneous rocks, recalculated by the method of Yoder and Tilley (1962) to Di, Hd, and Ac(Jd). + Pyroxenes from the new Borralan fenite; ■ from fenitized quartzites, Borralan (Woolley et al., 1972); ▲ from fenitized granite gneisses, Sokli (Vartianen and Woolley, 1976); ● from fenitized granite gneisses, Uganda (Sutherland, 1969).

Field for strongly alkaline (carbonatite suite) igneous rocks defined by data in Tyler and King (1967) and Rubie (1971) for E.Africa.

mildly alkaline (gabbro-monzonite-syenite trend, Morotu (Yagi, 1966).

Despite the absence of quartz, then, and bearing in mind the mineralogical similarity with the less equivocal fenitized quartzites reported before, a quartzite parent is preferred, and other possible parents may be refuted as follows:

Fucoid beds because of the low implied MK_2O and absence of biotite (Woolley et al., 1972); Lewisian gneiss because this fenite is unlike typical fenites formed from such gneisses, which usually comprise mainly microperthite with much more sodic pyroxene and magnesio-arfvedsonite (McKie, 1966); and Durness limestone both because of the absence of carbonates and because the mineralogy is dissimilar to metasomatic nepheline gneisses formed from limestones at Haliburton - Bancroft, the only well-documented xample of such an occurrence (Tilley, 1958).

This fenite, then, may represent a more extreme product of such replacement reactions as:

$$Na^+_{aq} + Fe^{3+}_{aq} + 3SiO_2 = \underset{\text{aegirine}}{NaFeSi_2O_6} + Si^{4+}_{aq}$$
quartzite

$$4Na^+_{aq} + 10(Mg,Fe)^{2+}_{aq} + 2Ca^{2+}_{aq} + 23SiO_2 = 2Na_2Ca(Mg,Fe)_5Si_8O_{22}(OH)_2 + 7Si^{4+}_{aq}$$
richterite

In this case some of the Mg and Ca may have come from decarbonation of Durness limestone rather than from the fenitizing magma, perhaps explaining the rather high Mg/(Mg+Fe^{2+}) of both amphibole and pyroxene (about 75 and 90% respectively allowing for Fe^{3+} in aegirine). Quartz then has been completely replaced,which may reflect either the greater metasomatic power of the pyroxene-hornblende syen tes relative to the pseudoleucite syenites, or perhaps restriction of fenite composition by CO_2 liberation at other localities(Rock, 1976), or, of course, lack of exposure of more extreme fenites produced by the pseudoleucite syenites. We can at least be certain, however, that the ultimate product of metasomatis doss not have the Ab-Or syenite minimum composition suggested by the three previous localities; it is difficult to envisage further metasomatism of the new fenite, which must therefore lie close to a highly individual end-product engineered by the unique and enigmatic geological conditions in this part of the Borralan complex.

REFERENCES

Leake (B.E.), 1968. Geol.Soc.Am.Spec.Pap.98
McKie (D.), 1966. In Tuttle (O.F.) and Gittins (J.), eds. Carbonatites (Wiley).
Matthews (D.W.) and Woolley (A.R.), 1976. Scott.J.Geol., in prep.
Rock (N.M.S.), 1976. Lithos, 9, 263-79
Rubie (D.C.), 1971. The Kisingiri Nephelinite Volcano. Th.D.Thesis, Leicester.
Sutherland (D.S.), 1969. Contrib.Mineral.Petrol. 24, 114-35
Tilley (C.E.), 1958. Q.J.Geol.Soc.Lond. 113, 323-60
Tyler (R.C.) and King (B.C.), 1967. Mineral.Mag. 36, 5-21
Vartianen (H.) and Woolley (A.R.), 1976. Bull.Geol.Surv.Finland, no.280
Woolley (A.R.), 1970. Geol.J. 7, 171-82
------ Symes (R.F.), and Elliott (C.J.), 1972. Mineral.Mag. 38, 819-30
Yagi (K.), 1966. Am.Mineral. 51, 976-1000
Yoder (H.S.) and Tilley (C.E.), 1962. J.Petrol. 3, 343-532

[Manuscript received 6 August 1976; revised 30 September 1976]

M8 | P.B.Moore: Mitridatite

Mitridatite: A remarkable octahedral sheet structure. Paul Brian Moore and Takaharu Araki, Department of the Geophysical Sciences, The University of Chicago, Chicago, Illinois 60637, U.S.A. Mitridatite, a natural phase, is a common product of weathering and oxidation of pre-existing ferrous phosphate minerals. This basic ferric phosphate occurs as dull green stains on granitic rocks, as colloidal to cryptocrystalline cement and nodules in marls, sandstones and other ferruginous sediments, and as a replacement of fossiliferous remains. It may be one of the more important inorganic phases in phosphatic soils (Moore, 1974). Rarity of suitable single crystal material has inhibited more detailed study of this phase.

Eventually a single crystal was found from the White Elephant pegmatite, near Custer, South Dakota. Another three years' work was devoted to unravelling its detailed crystal structure. We now report preliminary results on this study. R(hkℓ) = 0.11 for 1271 medium to strong reflections and 0.16 for 5449 reflections above background error. The essential correctness of the structure is attested by sharp contours on the Fourier synthesis and reasonable bond distances (Fe–O 1.88-2.10, P–O 1.49-1.60Å). Since 75 non-equivalent atoms occur in the asymmetric unit and since a substructure occurs, further refinement proceeds slowly. Structure cell data for mitridatite and related compounds appear in Table I. The atomic coordinate parameters are given in Table II.

Mitridatite possesses a remarkable structure, the knowledge of which permits us to relate it directly with other important oxysalt structure types. The underlying principle is a compact sheet of composition $[Fe_3^{3+}O_6(PO_4)_3]^{12-}$ (fig. 1). This sheet possesses trigonal pseudosymmetry, two-sided plane group p3lm, a = 11.25Å (= c of mitridatite). It is based on octahedral edge-sharing nonamers of general composition $M_9\phi_{26}$ where M is an octahedral center and ϕ is an octahedral vertex. These nonamers link at their extreme trigonal corners to form the octahedral sheet $M_9\phi_{33}$. At the center of each nonamer is a PO_4 tetrahedron (call it P(a)) which shares three of its corners with the octahedra. Removal of the three octahedra at the extreme trigonal corners (call them Fe(a)) leads to an octahedral cluster of composition $M_6\phi_{27}$. Including the central tetrahedron, the composition is PFe_6O_{28} (call these Fe atoms Fe(b)). This cluster (fig. 2) is topologically identical to the central girdle of the recently reported (D'Amour, 1976) $[P_{Mo_9O_{31}}(H_2O)_3]$ polyanion which was shown to be related to the well-known Keggin molecule. This polyanion can be partitioned to better show the relationship with mitridatite, that is $[PMo_6O_{28}Mo_3O_3(H_2O)_3]$.

To create the full mitridatite sheet based on the Fe_3 stoichiometry, two additional PO_4 tetrahedra (call them P(b)) link in the plane of the sheet and six additional tetrahedra (call them P(c)) above and below this plane, the latter each linking three of their corners to terminal oxygens above and below the sheet. Remaining are six oxo-anions which bridge three Fe atoms together. The fully assembled unit can be written $Fe(a)_3Fe(b)_6O_6(P(a)O_4)(P(b)O_4)_2(P(c)O_4)_6$. The Ca atoms and H_2O molecules form a broken sheet above and below the sheet already mentioned. Each Ca atom bonds to five oxygen atoms and two H_2O molecules, the latter defining a shared edge between the $CaO_5(H_2O)_2$ polyhedra. The polyhedron is made by adding a seventh vertex above a face of an octahedron. Finally, three water molecules occur which do not bond to any metals but participate in hydrogen bonding only. Thus, the asymmetric unit has the composition $Ca_6(H_2O)_6Fe_3^{3+}O_6(PO_4)_3]\cdot 3H_2O$.

A progressive sequence of sheets of increasing density (fig. 3) can now be conceived, starting with the iron phosphate derivative (= lusungite) of the familiar and important alunite structure (Wang *et al.*, 1965; Blount, 1974):

lusungite $[Fe(a)_3Fe(b)_6(OH)_{18}(P(c)O_4)_6]^{9-}$

↓

mitridatite $[Fe(a)_3Fe(b)_6O_6(P(a)O_4)(P(b)O_4)_2(P(c)O_4)_6]^{12-}$

↓

hypothetical $[Fe(a)_3Fe(b)_6O_6(P(a)O_4)_3(P(b)O_4)_3]^{3-}$

The hypothetical sheet is based on local oxygen cubic close-packing and can be condensed to the general formula $[M_3O_2(TO_4)_2]$, where T is a tetrahedron. It is known as a stable moiety in the crystal structure of chloritoid (Wedepohl, 1972), $Fe_2Al(OH)_4[Al_3O_2(SiO_4)_2]$. Among phosphates, a related sheet structure occurs in bermanite (Kampf and Moore, 1976), $Mn^{2+}(H_2O)_4[\square Mn_2^{3+}(OH)_2(PO_4)_2]$, where $\square$ is an ordered vacancy.

These relationships are of considerable interest since they point to structures which are highly stable and which transform according to rearrangements of oxygens in the sheets. These rearrangements admit a variety of tetrahedral decorations above, below and within such sheets. It is noted that in all these structures the octahedral centres, M, reside at the vertices of the familiar Kagomé net, a design of fundamental importance in inorganic structures, from alloys to the important spinel, Al_2MgO_4, structure type.

Knowledge of the mitridatite structure may shed light on the crystal chemistry of the curious phases betpakdalite and melkovite. These compounds occur as oxidation zone minerals associated with molybdenum sulfide deposits and their crystal chemistry was recently discussed (Skvortsova, 1972). Morphological and structure cell characters suggest a relationship with mitridatite. Although the formula $CaFe_2^{3+}(H_2O)_{14}[As_2Mo_5O_{24}]$ was proposed for betpakdalite, it can be rearranged isomorphically into a mitridatite-like formula, that is $Ca(H_2O)_8[\square_3Mo_5^{6+}Fe^{3+}O_6(FeO_4)(AsO_4)_2(OH)_{12}]$. Such an arrangement conserves local electrostatic neutrality since the three Fe(a) atoms in mitridatite are voided (= $\square$) and since the P(c)O_4 tetrahedra above and below the sheet are voided, and the free octahedral apices are bonded to $(OH)^-$ groups only. Table I summarizes the relationship; the agreement in the crystal cell data among the compounds is noteworthy. Confirmation of this relationship must await discovery of suitable single crystals for study.

References

Blount (A. M.), 1974. *Am. Mineral.* 59, 41-47.

D'Amour (H.), 1976. *Acta Crystallogr.* B32, 729-740.

Kampf (A. R.), and Moore (P.B.), 1976. *Am. Mineral.* 61, in the press.

Moore (P.B.), 1974, *Am. Mineral.* 59, 48-59.

Skvortsova (K. V.), Sidorenko (G. A.), Nesterova (Yu. S.), Arapova (G. A.), Dara (A. D.), and Rybakova (L. I.), 1972. *Internat. Geol. Rev.* 14, 473-480.

Wang (R.), Bradley (W. F.), and Steinfink (H.), 1965. *Acta Crystallogr.* 18, 249-252.

Wedepohl (K. H.)(ed.), 1972. *Handbook of Geochemistry*, II/3, Springer-Verlag (Berlin), 13-A-1 -13-A-24.

Table I. Crystal-chemical relationships between mitridatite and related phases*

Species	a(Å)	b(Å)	c(Å)	Degrees	Formula unit
Mitridatite	17.52	19.35	11.25	95.92°	$Ca_6(H_2O)_6[Fe_3^{3+}Fe_3^{3+}O_6(PO_4)(PO_4)_2(PO_4)_6]\cdot 3H_2O$
Robertsite	17.36	19.53	11.30	96.0	$Ca_6(H_2O)_6[Mn_3^{3+}Mn_3^{2+}O_6(PO_4)(PO_4)_2(PO_4)_6]\cdot 3H_2O$
Arseniosiderite	17.76	19.53	11.30	96.0	$Ca_6(H_2O)_6[Fe_3^{3+}Fe_3^{2+}O_6(AsO_4)(AsO_4)_2(AsO_4)_6]\cdot 3H_2O$
Betpakdalite	17.73	19.25	11.22	92.5°	$Ca(H_2O)_2[\square_3Mo_5^{6+}Fe^{3+}O_6(FeO_4)(AsO_4)_2(OH)_{12}]\cdot 6H_2O$
Melkovite	17.46	18.48	10.93	94.5°	$Ca(H_2O)_2[\square_3Mo_5^{6+}Fe^{3+}O_6(FeO_4)(PO_4)_2(OH)_{12}]\cdot 6H_2O$

*The cell parameters for the first three compounds are quoted from Moore, 1974 and the last two from Skvortsova *et al.*, 1972.

Table II. Mitridatite. Atomic coordinate parameters

Atom	x	y	z	Atom	x	y	z	Atom	x	y	z
Fe(1)	0.253	0.460	0.489	O(1)	0.024	0.282	0.140	O(25)	0.378	0.116	0.046
Fe(2)	.247	.037	.246	O(2)	.136	.232	.229	O(26)	.250	.068	.946
Fe(3)	.248	.055	.745	O(3)	.137	.347	.235	O(27)	.262	.194	.953
Fe(4)	.250	.200	.268	O(4)	.156	.285	.047	O(28)	.253	.123	.147
Fe(5)	.249	.221	.768								
Fe(6)	.251	.373	.250	O(5)	.020	.455	.627	O(29)	.379	.287	.543
Fe(7)	.255	.382	.754	O(6)	.141	.467	.506	O(30)	.262	.360	.438
Fe(8)	.254	.295	.021	O(7)	.137	.395	.693	O(31)	.254	.232	.444
Fe(9)	.244	.131	.523	O(8)	.140	.030	.198	O(32)	.256	.296	.630
Ca(1)	.084	.466	.299	O(9)	.013	.140	.640	O(33)	.131	.448	.975
Ca(2)	.084	.312	.842	O(10)	.136	.205	.733	O(34)	.250	.462	.876
Ca(3)	.080	.138	.343	O(11)	.133	.080	.730	O(35)	.238	.032	.563
Ca(4)	.419	.288	.208	O(12)	.131	.149	.545	O(36)	.262	.398	.074
Ca(5)	.418	.496	.664								
Ca(6)	.415	.156	.679	O(13)	.486	.472	.351	O(37)	.217	.118	.360
				O(14)	.364	.393	.260	O(38)	.276	.143	.686
P(1)	.108	.283	.160	O(15)	.359	.458	.477	O(39)	.282	.283	.184
P(2)	.106	.458	.634	O(16)	.358	.035	.767	O(40)	.221	.314	.860
P(3)	.104	.144	.667					O(41)	.222	.468	.311
P(4)	.396	.462	.337	O(17)	.486	.128	.401	O(42)	.280	.459	.666
P(5)	.391	.121	.382	O(18)	.354	.058	.301				
P(6)	.396	.303	.880	O(19)	.355	.118	.496	OW(1)	.493	.261	.405
				O(20)	.364	.181	.310	OW(2)	.493	.388	.656
P(7)	.214	.457	.999					OW(3)	.497	.064	.643
P(8)	.289	.126	.017	O(21)	.484	.302	.900	OW(4)	.497	.194	.182
P(9)	.290	.292	.519	O(22)	.366	.373	.810	OW(5)	.506	.474	.868
				O(23)	.363	.236	.794	OW(6)	.486	.127	.894
				O(24)	.367	.301	.022				
								OW(7)	.426	.455	.055
								OW(8)	.574	.373	.483
								OW(9)	.572	.217	.018

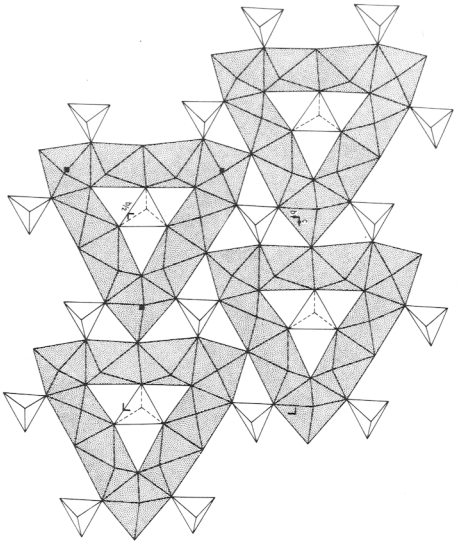

Fig. 1. Octahedral sheet (stippled) and intrasheet tetrahedra in mitridatite (unshaded) down the $\underset{\sim}{a}^*$-direction. The corner-linking tetrahedra above and below the sheet are not shown. Note the pseudo-trigonal symmetry of the structure.

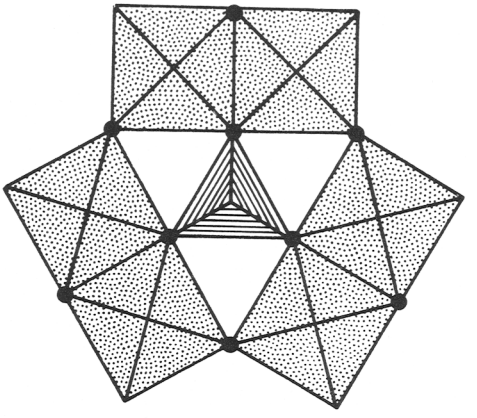

Fig. 2. The $[PFe_6O_{26}]$ cluster common to the crystal structure of mitridatite and the $[PMo_9O_{31}(H_2O)_3]$ polyanion.

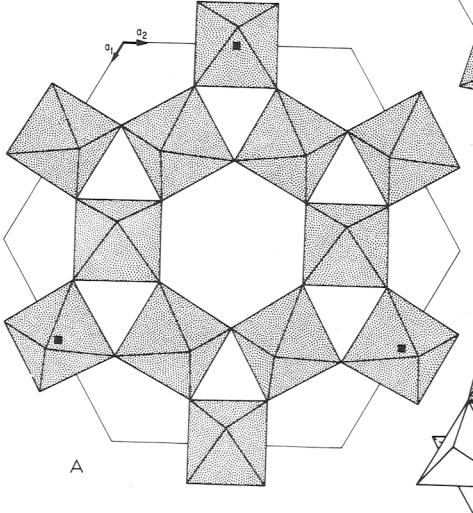

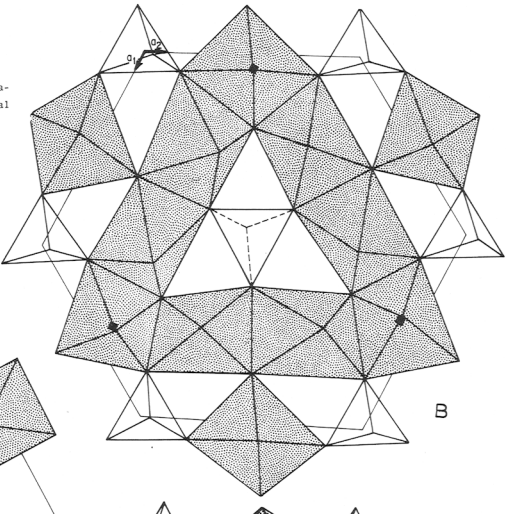

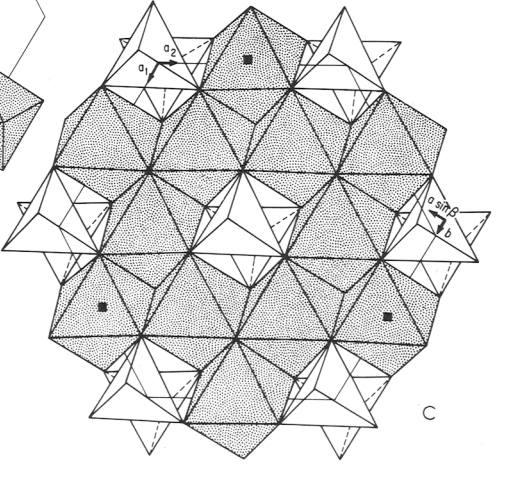

Fig. 3. Sequence of progressively condensed octahedral sheets in (a) the alunite structure type; (b) mitridatite, and (c) hypothetical $(Fe_9O_6(PO_4)_6)^{3-}$. For orientation, refer to the three solid squares on each diagram.